

GENUS ONE MINIMAL k -NOIDS AND SADDLE TOWERS IN $\mathbb{H}^2 \times \mathbb{R}$

JESÚS CASTRO-INFANTES AND JOSÉ M. MANZANO

ABSTRACT. For each $k \geq 3$, we construct a 1-parameter family of complete Alexandrov-embedded minimal surfaces in the Riemannian product space $\mathbb{H}^2 \times \mathbb{R}$ with genus 1 and k embedded ends asymptotic to vertical planes. We also obtain complete minimal surfaces with genus 1 and $2k$ ends in the quotient of $\mathbb{H}^2 \times \mathbb{R}$ by an arbitrary vertical translation. They all have dihedral symmetry with respect to k vertical planes, as well as finite total curvature $-4k\pi$. Finally, we provide examples of complete properly embedded minimal surfaces with infinitely many ends, each of them asymptotic to a vertical plane and with finite total curvature.

1. INTRODUCTION

The theory of complete minimal surfaces in $\mathbb{H}^2 \times \mathbb{R}$ with finite total curvature, i.e., those whose Gauss curvature is integrable, has received considerable attention during the last decade, mainly triggered by the work of Collin and Rosenberg [1]. The combined work of Hauswirth, Nelli, Sa Earp and Toubiana [4], and Hauswirth, Menezes and Rodríguez [3] shows that a complete minimal surface immersed in $\mathbb{H}^2 \times \mathbb{R}$ has finite total curvature if and only if it is proper, has finite topology and each of its ends is asymptotic to an admissible polygon, i.e., a curve homomorphic to \mathbb{S}^1 consisting of finitely-many alternating complete vertical and horizontal ideal geodesics, see [3]. Along with the previous work of Hauswirth and Rosenberg [5], this yields the following Gauss–Bonnet-type formula for a complete minimal surface Σ immersed in $\mathbb{H}^2 \times \mathbb{R}$ with finite total curvature:

$$\int_{\Sigma} K = 2\pi\chi(\Sigma) - 2\pi m = 2\pi(2 - 2g - k - m), \quad (1.1)$$

where g and k are the genus and the number of ends of Σ , respectively, $\chi(\Sigma) = 2 - 2g - k$ its Euler characteristic, K its Gauss curvature, and m is the total number of horizontal ideal geodesics contained in $\mathbb{H}^2 \times \{+\infty\}$, among all polygonal components associated with the ends of Σ . Observe that the union of all these polygons consists of m horizontal geodesics in $\mathbb{H}^2 \times \{+\infty\}$, m horizontal geodesics in $\mathbb{H}^2 \times \{-\infty\}$, and $2m$ vertical components in $\partial_{\infty}\mathbb{H}^2 \times \mathbb{R}$, whence the term $2\pi m$ in (1.1) can be understood as the sum of exterior angles of the asymptotic boundary of Σ .

Although this characterization is very satisfactory from a theoretical point of view, it seems tough in general to determine whether or not a given family of admissible

2010 *Mathematics Subject Classification*. Primary 53A10; Secondary 53C30.

Key words and phrases. Minimal surfaces, finite total curvature, minimal k -noids, saddle towers, conjugate construction.

polygons actually bounds a minimal surface, or if a given topological type can be realized by such a surface. In fact, there are not many examples of surfaces with finite total curvature in the literature. Let us highlight some of them in terms of the three parameters (g, k, m) appearing in (1.1):

- The simplest case is that of flat minimal surfaces, which must be vertical planes (i.e., of the form $\Gamma \times \mathbb{R}$, being $\Gamma \subset \mathbb{H}^2$ a complete geodesic) because of Gauss equation. In particular, vertical planes are the only complete minimal surfaces with finite total curvature and $(g, k, m) = (0, 1, 1)$, see also [6, Corollary 5].
- A minimal Scherk graph in $\mathbb{H}^2 \times \mathbb{R}$ is a minimal graph over a geodesic ideal polygon of \mathbb{H}^2 with $2a$ vertexes, $a \geq 2$, taking alternating limit values $+\infty$ and $-\infty$ on the sides of the polygon. A characterization of polygons carrying such a surface is analyzed in [12], in which case they have finite total curvature and satisfy $(g, k, m) = (0, 1, a)$. The case $a = 2$ gives rise to the only complete minimal surfaces with total curvature -2π , see [19, Theorem 4.1]. We can find as well the *twisted* Scherk minimal surfaces obtained by Pyo and Rodríguez [19] with $(g, k, m) = (0, 1, 2b + 1)$, $b \geq 1$, and total curvature $-4b\pi$ that are no longer graphs or bigraphs, some of which are embedded.
- Minimal k -noids constructed by Morabito and Rodríguez [14] (also by Pyo [18] in the symmetric case) have finite total curvature and k ends, $k \geq 2$, each of them asymptotic to a vertical plane. This corresponds to $g = 0$ and $k = m$ in (1.1).
- Horizontal catenoids ($k = 2$) are the only complete minimal surfaces immersed in $\mathbb{H}^2 \times \mathbb{R}$ with finite total curvature and $k = m = 2$, see [3, 4]. The family of minimal surfaces with finite total curvature and $k = m \geq 3$ is not hitherto well understood, not even in the case $g = 0$. The most general construction was given by Martín, Mazzeo and Rodríguez [10], who found properly embedded minimal surfaces with finite total curvature in $\mathbb{H}^2 \times \mathbb{R}$ of genus g and k ends asymptotic to vertical planes (and hence $m = k$), for arbitrary $g \geq 0$ and k arbitrarily large depending on g .

In this paper we provide highly symmetric examples with $g = 1$ and $m = k \geq 3$, which are hence conformally equivalent to a torus with k punctures. They can be seen as the counterpart in $\mathbb{H}^2 \times \mathbb{R}$ of the genus 1 minimal k -noids in \mathbb{R}^3 obtained by Mazet [11]. Outside a compact subset, they look like the minimal k -noids in [14, 18], though our surfaces are not globally embedded in general. Notice that there are no such examples with $k = 2$ due to the aforesaid uniqueness of horizontal catenoids [4]. Our main result can be stated as follows:

Theorem 1. *For each $k \geq 3$, there exists a 1-parameter family of properly Alexandrov-embedded minimal surfaces in $\mathbb{H}^2 \times \mathbb{R}$ with genus 1 and k ends, dihedrally symmetric with respect to k vertical planes and symmetric with respect to a horizontal plane. They have finite total curvature $-4k\pi$ and each of their ends is embedded and asymptotic to a vertical plane.*

The construction of these genus 1 minimal k -noids is based on a conjugate technique, in the sense of Daniel [2] and Hauswirth, Sa Earp and Toubiana [6]. Conjugation has been a fruitful technique to obtain constant mean curvature surfaces in $\mathbb{H}^2 \times \mathbb{R}$ and $\mathbb{S}^2 \times \mathbb{R}$, see [7, 8, 9, 11, 13, 14, 16, 17, 18] and the references therein. We begin by considering a solution to an improper Dirichlet problem [12, 15] in $\mathbb{H}^2 \times \mathbb{R}$ over an unbounded geodesic triangle $\Delta \subset \mathbb{H}^2$, a so-called Jenkins-Serrin problem. These solutions are minimal graphs over the interior of the triangle with prescribed finite and infinite values when one approaches the boundary Δ . The conjugate surface is another minimal graph in $\mathbb{H}^2 \times \mathbb{R}$ whose boundary is made of curves lying on totally geodesic surfaces, i.e., vertical and horizontal planes. Since there are isometric reflections across such planes in $\mathbb{H}^2 \times \mathbb{R}$, the conjugate surface can be extended to a complete surface under suitable conditions. In order to prescribe the symmetries stated in Theorem 1, we will encounter two period problems that will impose further restrictions on Δ and on the boundary values of the Jenkins-Serrin problem.

Our conjugate approach is inspired by the genus 1 minimal k -noids in \mathbb{R}^3 given by Mazet [11], and the mean curvature $\frac{1}{2}$ surfaces given by Plehnert [16]. It is important to remark that there exist technical dissimilarities resulting from the fact that the conjugate of a surface with mean curvature $\frac{1}{2}$ is a minimal surface in Heisenberg group Nil_3 , whose geometry is considerably different. Furthermore, our construction can be adapted to produce complete minimal surfaces invariant by an arbitrary vertical translation (i.e., in the direction of the factor \mathbb{R}), similar to the saddle towers given in [14]. Our surfaces have genus 1 in the quotient and they are not embedded in general.

Theorem 2. *For each $k \geq 3$ and each vertical translation T , there is a 1-parameter family of Alexandrov-embedded singly periodic minimal surfaces in $\mathbb{H}^2 \times \mathbb{R}$ invariant by T and dihedrally symmetric with respect to k vertical planes and a horizontal plane. They have finite total curvature $-4k\pi$, genus 1 and $2k$ vertical ends in the quotient of $\mathbb{H}^2 \times \mathbb{R}$ by T .*

Our analysis of the period problems will also allow us to find surfaces that are not invariant by a discrete group of rotations, but by discrete groups of parabolic or hyperbolic translations, which we will call *parabolic and hyperbolic ∞ -noids*, respectively. These surfaces have infinitely many ends, and we can guarantee many of the examples are properly embedded in the hyperbolic case. Although we will not state it explicitly, analogous surfaces can be obtained in the quotient by an arbitrary vertical translation in the spirit of Theorem 2.

Theorem 3. *There is a 2-parameter (resp. 1-parameter) family of properly embedded (resp. Alexandrov-embedded) minimal surfaces in $\mathbb{H}^2 \times \mathbb{R}$ with genus 0 and infinitely many ends, invariant by a discrete group of hyperbolic (resp. parabolic) translations. Each of their ends is embedded, asymptotic to a vertical plane, and has finite total curvature.*

The paper is organized as follows: In Section 2 we will briefly analyze some aspects of the conjugation of surfaces in $\mathbb{H}^2 \times \mathbb{R}$ that will be needed in the construction, and Section 3 will be devoted to fill the details in the proof of Theorems 1 and 2.

We will also discuss some open questions about the uniqueness and embeddedness of the constructed surfaces, as well as natural limits of the 1-parameter family of genus 1 k -noids. In the last part of the paper will prove Theorem 3.

Acknowledgement. The authors would like to express their gratitude to Magdalena Rodríguez for her valuable comments during the preparation of this manuscript. This research is supported by Spanish MINECO–FEDER research project MTM2017-89677-P. The first author is also supported by an FPU grant from the Spanish Ministry of Science and Innovation. The second author is also supported by the research program of the University of Granada.

2. PRELIMINARIES

Let Σ be a simply connected Riemannian surface. Given an isometric minimal immersion $X : \Sigma \rightarrow \mathbb{H}^2 \times \mathbb{R}$, Hauswirth, Sa Earp and Toubiana [6] proved the existence of another isometric minimal immersion $\tilde{X} : \Sigma \rightarrow \mathbb{H}^2 \times \mathbb{R}$ such that:

- (1) Both immersions induce the same angle function, i.e., $\nu = \langle N, \partial_t \rangle = \langle \tilde{N}, \partial_t \rangle$, where N and \tilde{N} stand for unit normal vector fields to X and \tilde{X} , respectively, and ∂_t is the unit vector field in $\mathbb{H}^2 \times \mathbb{R}$ in the direction of the factor \mathbb{R} .
- (2) The shape operators S and \tilde{S} of X and \tilde{X} , respectively, satisfy $\tilde{S} = JS$, where J is the $\frac{\pi}{2}$ -rotation in $T\Sigma$.
- (3) $\langle dX_p(u), \partial_t \rangle = -\langle Jd\tilde{X}_p(u), \partial_t \rangle$ for all $u \in T_p\Sigma$. In particular, the tangential projections of ∂_t satisfy $X^*T = J\tilde{X}^*\tilde{T}$, where $T = \partial_t - \nu N$ and $\tilde{T} = \partial_t - \nu \tilde{N}$.

The immersions X and \tilde{X} determine each other up ambient isometries, and are called *conjugate* immersions. In our construction, the initial surface $X(\Sigma)$ will be a vertical graph over a convex domain, namely a solution of a Jenkins-Serrin problem. This implies that $\tilde{X}(\Sigma)$ is also a vertical graph over another (possibly nonconvex) domain, due to the Krust-type theorem given by [6, Theorem 14]. Therefore, we can assume that both surfaces are embedded and will use the notation Σ and $\tilde{\Sigma}$ for the surfaces $X(\Sigma)$ and $\tilde{X}(\Sigma)$, respectively.

Although the conjugate surface $\tilde{\Sigma}$ is not explicit in general, one can obtain insightful information if the initial surface Σ has boundary consisting of geodesics intersecting at some vertexes. A curve $\Gamma \subset \Sigma$ is a horizontal (resp. vertical) geodesic in $\mathbb{H}^2 \times \mathbb{R}$ if and only if the conjugate curve $\tilde{\Gamma} \subset \tilde{\Sigma}$ lies in a vertical (resp. horizontal) totally geodesic surface of $\mathbb{H}^2 \times \mathbb{R}$ intersecting $\tilde{\Sigma}$ orthogonally along $\tilde{\Gamma}$. Furthermore, axial symmetry about Γ corresponds to mirror symmetry about $\tilde{\Gamma}$, which allows analytic continuation of Σ and $\tilde{\Sigma}$ across their boundaries. If the angles at the vertexes of $\partial\Sigma$ are integer divisors of π , then no singularity appears at such vertexes after successive reflections about the boundary components, and both surfaces can be extended to complete (possibly nonembedded) minimal surfaces. We refer to [7, 16, 13] for details.

However, most difficulties concerning the depiction of $\tilde{\Sigma}$, and in particular deciding whether or not it is embedded, show up when one tries to understand the behaviour of the conjugate of a vertical geodesic. We will now recall some properties on this matter which will be used later in Section 3. Let $\gamma : [a, b] \rightarrow \partial\Sigma$ be a vertical geodesic projecting onto a point in \mathbb{H}^2 , and denote by $\tilde{\gamma} : [a, b] \rightarrow \partial\tilde{\Sigma}$ the conjugate

curve, which can be assumed to lie in $\mathbb{H}^2 \times \{0\}$ after a vertical translation. Let κ_g be the geodesic curvature of $\tilde{\gamma}$ as a curve of $\mathbb{H}^2 \times \{0\}$ with respect to \tilde{N} . Note that \tilde{N} is conormal to $\tilde{\gamma}$ in $\mathbb{H}^2 \times \{0\}$ because $\tilde{\Sigma}$ intersects $\mathbb{H}^2 \times \{0\}$ orthogonally.

- (1) Since γ is vertical, we can express $N_{\gamma(t)} = \cos(\psi(t))E_1 + \sin(\psi(t))E_2$ along γ for some smooth function ψ , where $\{E_1, E_2, \partial_t\}$ represents a parallel orthonormal frame along γ . Then, $\psi'(t) = \kappa_g(t)$, see [9, 16].
- (2) In the half plane model $\mathbb{H}^2 = \{(x, y) \in \mathbb{R}^2 : y > 0\}$, whose metric is given by $y^{-2}(dx^2 + dy^2)$, consider the orthonormal frame $\{e_1 = -y\partial_x, e_2 = -y\partial_y\}$ (observe that e_1 is tangent to a foliation by horocycles). Let $\theta(t)$ be a smooth angle between $\tilde{\gamma}(t)$ and e_1 , i.e., a smooth function satisfying $\gamma' = \cos(\theta)e_1 + \sin(\theta)e_2$. A similar computation to that in [16, Proposition 4.8] with $H = 0$ rather than $H = \frac{1}{2}$ yields the identity

$$\theta'(t) = \kappa_g(t) + \cos(\theta(t)) = \psi'(t) + \cos(\theta(t)). \quad (2.1)$$

3. CONSTRUCTION OF GENUS 1 SADDLE TOWERS AND k -NOIDS

The first part of this section is devoted to prove Theorems 1 and 2. The arguments leading to these results are based on a conjugate construction that depends on a parameter $0 < l \leq \infty$ that will be fixed henceforth. The case $0 < l < \infty$ gives the saddle towers whose fundamental pieces lie in a slab of height l , whereas the case $l = \infty$ gives rise to the k -noids. Although a limit argument for $l \rightarrow \infty$ would imply the latter (as in [14]) we will discuss both cases together.

3.1. The conjugate construction. Let Δ a geodesic triangle with sides ℓ_1 , ℓ_2 and ℓ_3 , and opposite vertexes p_1 , p_2 and p_3 . Assume that Δ is acute and the length of ℓ_2 is given by the aforesaid parameter $l \in (0, \infty]$, and hence p_1 becomes ideal if $l = \infty$. Therefore Δ is determined by the length a of ℓ_1 and by the angle φ at p_2 . Given $b \in \mathbb{R}$, consider the unique solution $\Sigma(a, \varphi, b)$ to the Jenkins-Serrin problem over Δ with boundary values b along ℓ_1 , $+\infty$ along ℓ_2 , and 0 along ℓ_3 . Existence and uniqueness of such a solution is guaranteed under these boundary conditions, see [12] and the references therein. In particular, the interior of $\Sigma(a, \varphi, b)$ is a minimal graph over Δ whose boundary consists of two horizontal geodesics h_1 and h_3 lying in $\mathbb{H}^2 \times \{b\}$ and $\mathbb{H}^2 \times \{0\}$, respectively, and three vertical geodesics v_1 , v_2 and v_3 projecting onto p_1 , p_2 and p_3 , respectively. Note that v_3 is an ideal vertical geodesic provided that $l = \infty$. The boundary of $\Sigma(a, \varphi, b)$ also contains an horizontal ideal geodesic $h_2 \subset \mathbb{H}^2 \times \{\infty\}$ projecting onto ℓ_2 . Since $\Delta \subset \mathbb{H}^2$ is convex, the conjugate minimal surface $\tilde{\Sigma}(a, \varphi, b) \subset \mathbb{H}^2 \times \mathbb{R}$ is a graph over some domain $\tilde{\Delta} \subset \mathbb{H}^2$ due to the Krust-type theorem in [6].

The conjugate curves \tilde{h}_1 and \tilde{h}_3 lie in vertical planes, and the conjugate curves \tilde{v}_1 and \tilde{v}_2 lie in horizontal planes. The conjugate curve \tilde{h}_2 is an ideal vertical geodesic of length l , and hence \tilde{v}_3 becomes an ideal horizontal geodesic if $l = \infty$, see Figure 3.1. We would like \tilde{v}_2 and \tilde{v}_3 to be contained in the same horizontal plane, as well as the prolongations of the projections of \tilde{h}_1 and \tilde{h}_3 to intersect at an angle of $\frac{\pi}{k}$. Such a configuration would lead to the desired construction of saddle towers and k -noids, so one needs to solve the following period problems inspired by the arguments in [16]:

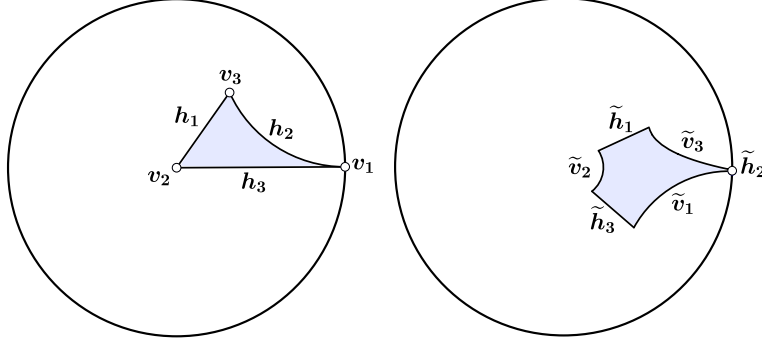


FIGURE 1. Projections to \mathbb{H}^2 of the graphs $\Sigma(a, \varphi, b)$ and $\tilde{\Sigma}(a, \varphi, b)$ in the case $l = \infty$. White dots represent vertical geodesics contained in the boundaries.

- (1) **First period problem.** Let $p_1(a, \varphi, b)$ be the difference of heights of the horizontal curves \tilde{v}_2 and \tilde{v}_3 , i.e., the difference of heights of the endpoints of \tilde{h}_1 . Parametrizing $\tilde{h}_1 : [t_1, t_2] \rightarrow \mathbb{H}^2 \times \mathbb{R}$ with unit-speed, and writing in components $h_1 = (\beta, z) \in \mathbb{H}^2 \times \mathbb{R}$, we get

$$p_1(a, \varphi, b) = z(t_1) - z(t_2) = - \int_{\tilde{h}_1} \langle \tilde{h}'_1, \partial_t \rangle = \int_{h_1} \langle Jh'_1, \partial_t \rangle = \int_{h_1} \langle \eta, \partial_t \rangle,$$

where η is a unit conormal vector to $\Sigma(a, \varphi, b)$ along h_1 . The sign of η is irrelevant since we seek $p_1(a, \varphi, b) = 0$, though will choose the inward-pointing conormal.

- (2) **Second period problem.** In the half plane model, up to an ambient isometry, we can assume that \tilde{h}_3 is contained in the vertical plane $\{x = 0\}$, $\tilde{v}_2 : [0, b] \rightarrow \mathbb{H}^2 \times \mathbb{R}$ has unit speed and is contained in the horizontal plane $\{t = 0\}$ with endpoints $\tilde{v}_2(0) = (0, 1, 0)$ and $\tilde{v}_2(b) = (x_0, y_0, 0)$ for some $(x_0, y_0) \in \mathbb{H}^2$.

Let $\theta(t)$ be the angle that $\tilde{v}'_2(t)$ makes with the vector field $-\partial_x$ at $\tilde{v}_2(t)$, and assume that $\theta_0 = \theta(b) \in (0, \pi)$ and $x_0 < 0$ (these assumptions will be satisfied in view of Lemma 3). Let γ be the geodesic ray starting at (x_0, y_0) , perpendicular to \tilde{v}_2 as in Figure 2, which is parametrized by

$$\gamma : [\pi - \theta_0, \pi) \rightarrow \mathbb{H}^2, \quad \gamma(t) = \left(x_0 - y_0 \frac{\cos(t) + \cos(\theta_0)}{\sin(\theta_0)}, y_0 \frac{\sin(t)}{\sin(\theta_0)} \right),$$

If γ intersects the y -axis, then it is easy to check that the cosine of the angle at the intersection is given by

$$p_2(a, \varphi, b) = \cos(\theta_0) - \frac{x_0 \sin(\theta_0)}{y_0}.$$

We will prove in Lemma 3 that if $p_1(a, \varphi, b) = 0$ and $p_2(a, \varphi, b) = \cos(\frac{\pi}{k})$ for some $k \geq 3$, then γ and the y -axis do intersect and the angle at the intersection is $\frac{\pi}{k}$.

The uniqueness of solution of the Jenkins-Serrin problem implies that $\tilde{\Sigma}(a, \varphi, b)$ depends smoothly on the parameters (a, φ, b) in the sense that, given a sequence (a_n, b_n, φ_n) converging to some (a, φ, b) , the sequence of surfaces with boundary $\tilde{\Sigma}(a_n, b_n, \varphi_n)$ converges in the \mathcal{C}^k -topology to $\tilde{\Sigma}(a, \varphi, b)$ for all $k \geq 0$. This follows

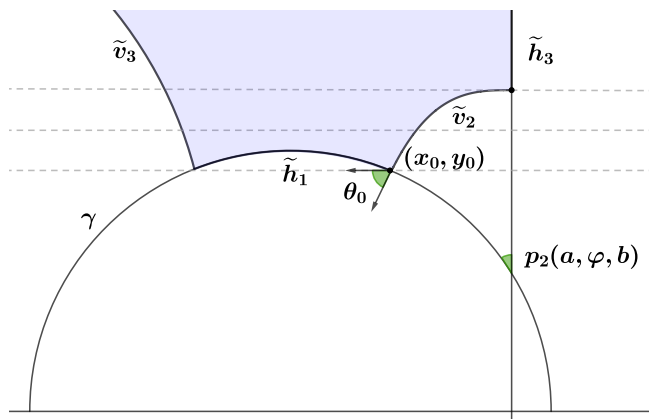


FIGURE 2. Second period $p_2(a, \varphi, b)$ and the angle θ_0 the curve \tilde{v}_2 makes with respect to the horocycle foliation at (x_0, y_0) . Observe that the surface $\tilde{\Sigma}(a, \varphi, b)$ projects onto the shaded region.

from standard convergence arguments for minimal graphs along with the continuity of the conjugation, see [14, Proposition 2.10] for a detailed proof.

3.2. Solving the period problems. In the sequel we will assume that b is any real number and (a, φ) lies in the domain

$$\Omega = \left\{ (a, \varphi) \in \mathbb{R}^2 : 0 < \varphi < \frac{\pi}{2}, 0 < a < a_{\max}(\varphi) \right\},$$

where $a = a_{\max}(\varphi)$ is the unique solution to the equation

$$\tanh(l) = \frac{\cosh(a) - 1}{\sinh(a) \cos(\varphi)}. \quad (3.1)$$

Remark 1. This means that the angle of Δ at p_3 is always greater than φ and then the isosceles triangle Δ_0 with vertices p_2, p_3, p_4 , and $d(p_1, p_4) = d(p_2, p_4) = l$ intersects Δ as in Figure 3. If $l = \infty$, then we assume that $\tanh(l) = 1$ in Equation (3.1) and the vertex p_4 is ideal. The restriction $(a, \varphi) \in \Omega$ will be used in Lemma 2 to compare $\Sigma(a, \varphi, b)$ with a surface solving a Jenkins-Serrin problem over Δ_0 and solve the first period problem. Similar arguments to those in Lemma 2 show that if $a > a_{\max}(\varphi)$, then the first period problem has no solution, which makes it natural to restrict the parameters to the domain Ω .

Lemma 1. $p_1 : \Omega \times \mathbb{R}^+ \rightarrow \mathbb{R}$ is a continuous and decreasing function with respect to the third argument b .

Proof. Consider two surfaces $\Sigma_1 = \Sigma(a, \varphi, b_1)$ and $\Sigma_2 = \Sigma(a, \varphi, b_2)$ with $b_1 \leq b_2$. Let us translate each Σ_i vertically so that it takes zero value along ℓ_1 and $-b_i$ along ℓ_3 . Then the surface Σ_1 is a barrier lying above Σ_2 and we can compare the vertical components of the inward-pointing conormals $\langle \eta_2, \partial_t \rangle \leq \langle \eta_1, \partial_t \rangle$, hence

$$p_1(a, \varphi, b_2) = \int_{h_1} \langle \eta_2, \partial_t \rangle \leq \int_{h_1} \langle \eta_1, \partial_t \rangle = p_1(a, \varphi, b_1). \quad \square$$

Lemma 2. There exists a unique function $f : \Omega \rightarrow \mathbb{R}_+$ such that $p_1(a, \varphi, f(a, \varphi)) = 0$ for all $(a, \varphi) \in \Omega$. Furthermore,

- (a) f is a continuous function;
 (b) given $\varphi_0 \in (0, \frac{\pi}{2})$,

$$\lim_{a \rightarrow a_{\max}(\varphi_0)} f(a, \varphi_0) = \infty, \quad \lim_{(a, \varphi) \rightarrow (0, \varphi_0)} f(a, \varphi) = 0.$$

Proof. Fix $(a, \varphi) \in \Omega$. Let p_4 be a point in the bisector of the segment ℓ_1 with $d(p_1, p_4) = d(p_2, p_4) = l$, such that the triangle Δ_0 with vertexes p_1 , p_2 and p_4 lies on the same side of ℓ_1 as Δ , see Figure 3. Let $\Sigma_0(b)$ be the unique solution to the Jenkins-Serrin problem over the triangle Δ_0 with values b along p_2p_3 , $+\infty$ along p_3p_4 , and $-\infty$ along p_2p_4 . Since $(a, \varphi) \in \Omega$, then $\Delta \cap \Delta_0 \subset \mathbb{H}^2$ is a bounded geodesic triangle with vertexes p_2 , p_3 and $q \in \ell_3$, see Remark 1. If b is sufficiently large, then $\Sigma(a, \varphi, b) \cap \Sigma_0(b) = h_1 \cup v_2 \cup v_3$, and $\Sigma_0(b)$ is a barrier lying above $\Sigma(a, \varphi, b)$.

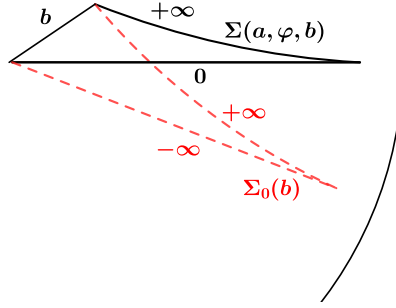


FIGURE 3. The Jenkins-Serrin problems in \mathbb{H}^2 solved by the surfaces $\Sigma(a, \varphi, b)$ and $\Sigma_0(b)$, the latter in dashed line, for some $l < \infty$.

We can compare the vertical component of the inward-pointing conormal η of $\Sigma(a, \varphi, b)$ with the vertical component of the inward-pointing conormal η_0 of $\Sigma_0(b)$ along the curve h_1 as in Lemma 1. By the boundary maximum principle for minimal surfaces, we get the strict inequality $\langle \eta, \partial_t \rangle < \langle \eta_0, \partial_t \rangle$ along h_1 , and hence

$$p_1(a, \varphi, b) = \int_{h_1} \langle \eta, \partial_t \rangle < \int_{h_1} \langle \eta_0, \partial_t \rangle = 0. \quad (3.2)$$

On the other hand, due to the continuity of $\Sigma(a, \varphi, b)$ with respect to the parameters (a, φ, b) , the surfaces $\Sigma(a, \varphi, b)$ converge to $\Sigma(a, \varphi, 0)$ as $b \rightarrow 0$. We have that $p_1(a, \varphi, 0) > 0$ since we can compare the inward-pointing conormals of $\Sigma(a, \varphi, 0)$ and the horizontal slice $\mathbb{H}^2 \times \{0\}$ along h_1 , as in the above argument. By the continuity and monotonicity of p_1 with respect to b proved in Lemma 1, there exist a unique $b_0 \in \mathbb{R}^+$ such that $p_1(a, \varphi, b_0) = 0$. Hence this defines univocally $f(a, \varphi) = b_0$. The continuity of f is a consequence of its uniqueness. If (a_n, φ_n) and (a'_n, φ'_n) are two sequences in Ω converging to some $(a_\infty, \varphi_\infty) \in \Omega$ such that, after passing to a subsequence, $f(a_n, \varphi_n) \rightarrow b_\infty$ and $f(a'_n, \varphi'_n) \rightarrow b'_\infty$, then both $p_1(a_\infty, \varphi_\infty, b_\infty) = p_1(a_\infty, \varphi_\infty, b'_\infty) = 0$, whence $b_\infty = b'_\infty$, and item (a) is proved.

As for the first limit in item (b), assume by contradiction that there is a sequence $a_n \rightarrow a_{\max}(\varphi_0)$ such that $f(a_n, \varphi_0)$ converges, after passing to a subsequence, to some $b_\infty \in [0, +\infty)$. The surfaces $\Sigma_0(b_\infty)$ and $\Sigma(a_{\max}(\varphi_0), \varphi, b_\infty)$ are minimal graphs over the triangle Δ_0 with value b_∞ along ℓ_1 , and their inward-pointing

conormals can be compared again along h_1 , which clearly contradicts the fact that both surfaces have zero period.

We will compute the limit as (a, φ) approaches $(0, \varphi_0)$ again by contradiction, so let us assume that there is a sequence (a_n, φ_n) tending to $(0, \varphi_0)$ such that (after passing to a subsequence) $f(a_n, \varphi_n) \rightarrow b_\infty$, with $b_\infty \in (0, +\infty]$. Let us translate the surfaces $\Sigma(a_n, \varphi_n, f(a_n, \varphi_n))$ vertically so that they take zero value along ℓ_1 and $-f(a_n, \varphi_n)$ along ℓ_3 . Since $a_n \rightarrow 0$, we can blow up the surface and the metric of $\mathbb{H}^2 \times \mathbb{R}$ in such a way a_n is equal to 1. The new sequence of rescaled surfaces converges in the \mathcal{C}^k -topology for all k to a minimal surface Σ_∞ in Euclidean space \mathbb{R}^3 . This surface Σ_∞ is a graph over a domain of \mathbb{R}^2 bounded by three lines $\ell_{1\infty}$, $\ell_{2\infty}$ and $\ell_{3\infty}$ such that $\ell_{2\infty}$, $\ell_{3\infty}$ are parallel and $\ell_{1\infty}$ makes an angle of φ_0 with $\ell_{2\infty}$. Moreover, Σ_∞ takes values $+\infty$ along $\ell_{2\infty}$, $-\infty$ along $\ell_{3\infty}$ (since $b_\infty > 0$), and 0 along $\ell_{1\infty}$. Let us consider Σ_0 the helicoid of \mathbb{R}^3 with axis $\ell_{1\infty}$ which is a graph over half a slab of \mathbb{R}^2 as depicted in Figure 4. Since $0 < \varphi_0 < \frac{\pi}{2}$, we deduce that the helicoid lies above the surface Σ_∞ , and hence we can compare their conormals along $\ell_{1\infty}$ and conclude that the period of Σ_∞ cannot be zero, which contradicts that each of the surfaces $\Sigma(a_n, \varphi_n, f(a_n, \varphi_n))$ has zero period. \square

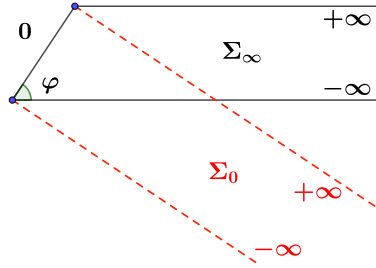


FIGURE 4. The limit Σ_∞ and the helicoid Σ_0 in \mathbb{R}^3 , which a graph over the halfslab with boundary the dashed half-lines.

Lemma 3. *Let $\varphi_0 \in (0, \frac{\pi}{2})$ and $a \in (0, a_{\max}(\varphi_0))$.*

- (a) *The conditions $x_0 < 0$ and $0 < \theta_0 < \pi$ hold true.*
- (b) *If the curve γ intersects the positive y -axis with angle δ , then $\delta < \varphi_0$, in which case $p_2(a, \varphi_0, f(a, \varphi_0)) = \cos(\delta)$.*
- (c) *If $p_2(a, \varphi_0, f(a, \varphi_0)) = \cos(\delta)$ for some $\delta \in (0, \varphi_0)$, then γ intersects the positive y -axis with angle δ .*
- (d) *If $p_2(a, \varphi_0, f(a, \varphi_0)) = 1$, then γ and the y -axis are asymptotic geodesics intersecting at the ideal point $(0, 0)$.*

Furthermore,

$$\lim_{a \rightarrow 0} p_2(a, \varphi_0, f(a, \varphi_0)) = \cos(\varphi_0), \quad \lim_{a \rightarrow a_{\max}(\varphi_0)} p_2(a, \varphi_0, f(a, \varphi_0)) = +\infty.$$

Proof. We will prove item (a) reasoning by contradiction. Assume that $x_0 \geq 0$ for some value of $a \in (0, a_{\max}(\varphi_0))$. Then there is a first value t_0 such that $\tilde{v}_2(t_0)$ lies in the y -axis, so the curve \tilde{v}_2 between 0 and t_0 together with a segment of the y -axis enclose a bounded domain $U \subset \mathbb{H}^2 \times \{0\}$. Gauss-Bonnet formula applied to U yields $0 > -\text{area}(U) > \frac{\pi}{2} - \varphi_0$, in contradiction with the fact that $\varphi_0 \in (0, \frac{\pi}{2})$.

Next let us observe that the inequality $\theta_0 > 0$ is clearly satisfied because of the convexity of the curve \tilde{v}_2 , so let us assume that $\theta_0 \geq \pi$ for some value of $a \in (0, a_{\max}(\varphi_0))$. Again, there is a first value of t_0 such that $\theta(t_0) = \pi$, which implies that the normal geodesic to \tilde{v}_2 at t_0 is a straight line parallel to the y -axis. Let us now consider the domain $U \subset \mathbb{H}^2 \times \{0\}$ enclosed by this line together with an arc of \tilde{v}_2 , so that Gauss-Bonnet formula applied to U yields the same contradiction $0 > -\text{area}(U) > \frac{\pi}{2} - \varphi_0$, which finishes the proof of item (a).

As for item (b), if γ intersects the y -axis with angle δ , then there is a region $U \subset \mathbb{H}^2$ bounded by γ , \tilde{v}_2 and the y -axis, in which Gauss-Bonnet formula gives the inequality $0 > -\text{area}(U) > \delta - \varphi_0$, which is equivalent to $\delta < \varphi_0$. We compute the cosine of the angle δ as

$$\cos(\delta) = \frac{\langle \gamma', (0, -1) \rangle}{|\gamma'|} = \cos(\theta_0) - \frac{x_0 \sin(\theta_0)}{y_0} = p_2(a, \varphi_0, f(a, \varphi_0)).$$

As for items (c) and (d), the intersection of γ and the x -axis occurs at the point

$$\gamma(\pi) = \left(x_0 + y_0 \frac{1 - \cos(\theta_0)}{\sin(\theta_0)}, 0 \right). \quad (3.3)$$

If $p_2(a, \varphi_0, f(a, \varphi_0)) = \cos(\theta_0) - \frac{x_0 \sin(\theta_0)}{y_0} = \cos(\delta) \in (0, 1)$ then the first component in (3.3) is positive and then γ intersects the y -axis, and the angle can be computed as in item (b). If $p_2(a, \varphi_0, f(a, \varphi_0)) = 1$, then the first component in (3.3) vanishes, so that γ and the y -axis converge to the ideal point $(0, 0)$.

To finish the proof, let us analyze the limits. First of all, observe that integrating (2.1) from 0 to b , computed along the horizontal curve \tilde{v}_2 , and taking into account that $\theta(0) = \psi(0) = 0$, $\theta(b) = \theta_0$ and $\psi(b) = \varphi_0$, we get the estimate

$$\theta_0 - \varphi_0 = \int_0^b \cos(\theta(s)) ds \leq b. \quad (3.4)$$

In particular, if b tends to zero, one has $\theta_0 \rightarrow \varphi_0$, and also $(x_0, y_0) \rightarrow (0, 1)$ since the length of \tilde{v}_2 goes to zero. This means that the first component in (3.3) is positive, i.e., $\gamma(\pi)$ and (x_0, y_0) lie at opposite sides of the y -axis for b small enough, in which case γ intersects the positive y -axis at some point. By Lemma 2, if $a \in (0, a_{\max}(\varphi_0))$ tends to zero, then $b = f(a, \varphi_0)$ also tends to zero and

$$\lim_{a \rightarrow 0} p_2(a, f(a, \varphi_0), \varphi_0) = \lim_{a \rightarrow 0} \left(\cos(\theta_0) - \frac{x_0 \sin(\theta_0)}{y_0} \right) = \cos(\varphi_0).$$

As for the limit $a \rightarrow a_{\max}(\varphi_0)$, let $(a_n, \varphi_0) \in \Omega$ be a sequence with $a_n \rightarrow a_{\max}(\varphi_0)$. Lemma 2 tells us that $f(a_n, \varphi_0) \rightarrow +\infty$, so the surfaces $\Sigma(a_n, \varphi_0, f(a_n, \varphi_0))$ converge to a solution Σ_∞ to a Jenkins-Serrin problem over an isosceles triangle with values 0 along the unequal side and $+\infty$ and $-\infty$ along the other sides.

- If $l < \infty$, the conjugate surfaces converge to $\tilde{\Sigma}_\infty$, a half of the fundamental piece of a symmetric saddle tower with four edges, see [14]: the curves \tilde{v}_{1n} converge to a complete horizontal curve $\tilde{v}_{1\infty}$, and we can assume that \tilde{h}_{1n} are contained in the plane $\{x = 0\}$ and \tilde{v}_{2n} and \tilde{v}_{3n} are contained in the plane $\{t = 0\}$ after suitable ambient isometries. In this case, $\theta_{0n} \rightarrow \theta_{0\infty} = \frac{\pi}{2}$ as $n \rightarrow \infty$ and the points (x_{0n}, y_{0n}) converge to the ideal point $(x_{0\infty}, 0)$ with $x_{0\infty} < 0$. This gives an infinite value for p_2 so, in view of (3.3), we

deduce that γ_n does not intersect the positive y -axis for n large enough, and $p_2(a_n, \varphi_0, f(a_n, \varphi_0)) \rightarrow +\infty$.

- If $l = \infty$, then it is also well known [14, 18] that the conjugate surfaces converge to $\tilde{\Sigma}_\infty$, a quarter of a horizontal catenoid: the curves \tilde{v}_{1n} converge to a complete ideal geodesic $\tilde{v}_{1\infty} \subset \mathbb{H}^2 \times \{+\infty\}$, and we can reason as in the case $l < \infty$. \square

Proof of Theorems 1 and 2. Let $k \geq 3$. For each $\frac{\pi}{k} < \varphi < \frac{\pi}{2}$, Lemma 3 ensures that $p_2(a, \varphi, f(a, \varphi))$ tends to $\cos(\varphi)$ when $a \rightarrow 0$ and tends to $+\infty$ when $a \rightarrow a_{\max}(\varphi)$. Since $\cos(\varphi) < \cos(\frac{\pi}{k})$ and p_2 is continuous, there exists some $a_\varphi \in (0, a_{\max}(\varphi))$ such that $p_2(a_\varphi, \varphi, f(a_\varphi, \varphi)) = \cos(\frac{\pi}{k})$, though it might not be unique. Therefore, we deduce from item (c) of Lemma 3 that $\tilde{\Sigma}(a_\varphi, \varphi, f(a_\varphi, \varphi))$ solves both period problems. On the one hand, observe that $\tilde{\Sigma}(a_\varphi, \varphi, f(a_\varphi, \varphi))$ has total Gauss curvature $-\pi$, which follows from a standard application of Gauss–Bonnet formula to a sequence of compact minimal graphs of total curvature $-\pi$ converging monotonically to $\tilde{\Sigma}(a_\varphi, \varphi, f(a_\varphi, \varphi))$, see [1, Remark 7] (note that minimal surfaces in $\mathbb{H}^2 \times \mathbb{R}$ have negative Gauss curvature, so there are no integrability issues). On the other hand, since $\Sigma(a, \varphi, f(a, \varphi))$ becomes vertical when one approaches the side ℓ_2 , the length of the ideal vertical geodesic \tilde{h}_2 coincides with the parameter l representing the length of the side ℓ_2 of the initial triangle Δ . In particular, the difference of heights between the horizontal curves \tilde{v}_1 and \tilde{v}_3 is equal to l .

By successive mirror reflections across the planes containing the boundary components of $\tilde{\Sigma}(a_\varphi, \varphi, f(a_\varphi, \varphi))$, we obtain a complete properly Alexandrov-embedded minimal surface $\tilde{\Sigma}_\varphi \subset \mathbb{H}^2 \times \mathbb{R}$.

- If $l < \infty$, then the composition of the reflections with respect to the horizontal planes containing \tilde{v}_1 and \tilde{v}_3 is a vertical translation T of length $2l$. Thus, $\tilde{\Sigma}_\varphi$ induces a surface in the quotient space $\mathbb{H}^2 \times \mathbb{S}^1$ by T with total Gauss curvature $-4k\pi$, since it consists of $4k$ pieces isometric to $\tilde{\Sigma}(a_\varphi, \varphi, f(a_\varphi, \varphi))$. Finally, the surface in the quotient has $2k$ ends, each of them asymptotic to an ideal vertical geodesic circle $\{q\} \times \mathbb{S}^1$ for some $q \in \partial_\infty \mathbb{H}^2$.
- If $l = \infty$, then the curve \tilde{v}_3 becomes ideal, and we only need to reflect once about a horizontal plane, i.e., the plane containing \tilde{v}_1 . Since we still need $4k$ copies of $\tilde{\Sigma}(a_\varphi, \varphi, f(a_\varphi, \varphi))$, the total curvature in this case is $-4k\pi$.

Each end of $\tilde{\Sigma}_\varphi$ has asymptotic boundary consisting of four complete ideal geodesics: two horizontal ones obtained from \tilde{v}_1 , and two vertical ones obtained from \tilde{h}_2 . In particular, such an end is asymptotic to a vertical plane and it is contained in four copies of $\tilde{\Sigma}(a_\varphi, \varphi, f(a_\varphi, \varphi))$. We claim that the subset of $\tilde{\Sigma}_\varphi$ formed by these four copies is a symmetric bigraph, so the end is embedded in particular. This claim follows from the fact that two of these four pieces come from $\Sigma(a_\varphi, \varphi, f(a_\varphi, \varphi))$ and its axially symmetric surface with respect to h_2 , which project into a convex quadrilateral of \mathbb{H}^2 . Therefore, the Krust-type result guarantees that the conjugate $\tilde{\Sigma}(a_\varphi, \varphi, f(a_\varphi, \varphi))$, together with its mirror symmetric surface with respect to the plane containing \tilde{h}_2 , form an embedded graph. The other two copies needed to produce the end are their symmetric ones with respect to the horizontal plane containing \tilde{v}_2 and \tilde{v}_3 . \square

Remark 2. It is important to notice that we are not proving the uniqueness of the surface Σ_φ in the proof above. This would be automatically true if we could show that the second period $p_2(a, \varphi, f(a, \varphi))$ is strictly increasing in the parameter a , though a comparison of the surfaces for different values of a seems to be difficult, since we do not even know if the function f solving the first period problem is monotonic.

As φ approaches $\frac{\pi}{k}$, the value a_φ solving the two period problems in the proof of Theorems 1 and 2 goes to zero, and the surface $\tilde{\Sigma}_\varphi$ converges, after rescaling, to a genus 1 minimal k -noid in \mathbb{R}^3 (as in item (b) of Lemma 2). Moreover, when φ approaches $\frac{\pi}{2}$, the surface Σ_φ converges to an open subset of a helicoid in \mathbb{R}^3 after rescaling, and it follows that the conjugate surfaces $\tilde{\Sigma}_\varphi$ must converge a quarter of a catenoid in \mathbb{R}^3 (the curve \tilde{h}_1 converges to half of the neck of such catenoid).

3.3. The embeddedness problem. In the proof of Theorems 1 and 2, it is shown that the conjugate piece $\tilde{\Sigma}(a, \varphi, f(a, \varphi))$ is a graph over the domain $\tilde{\Delta} \subset \mathbb{H}^2$. But it can happen that when we reflect the surface $\tilde{\Sigma}(a, \varphi, f(a, \varphi))$ over the vertical plane containing \tilde{h}_1 , the resulting surface is not embedded since the reflected curve of \tilde{v}_3 might intersect the curve \tilde{v}_3 . In fact, the family of examples with k ends converges to a genus 1 minimal k -noid in \mathbb{R}^3 after blow up, see also [11], as in item (b) of Lemma 2. Therefore, there do exist non-embedded examples of k -noids and saddle towers with genus 1 in $\mathbb{H}^2 \times \mathbb{R}$ for all $k \geq 3$.

A condition that guarantees the embeddedness of the surface is that the reflected surface over the vertical plane containing \tilde{h}_1 is embedded. By the Krust type property we can ensure this condition if the initial surface $\Sigma(a, \varphi, f(a, \varphi))$ extended by the reflection over the geodesic h_1 is still a graph over a convex domain. This occurs when the angle of the triangle Δ at the vertex p_3 is less than or equal to $\frac{\pi}{2}$. Elementary hyperbolic geometry shows that this is equivalent to

$$\tanh(a) > \tanh(l) \cos(\varphi). \quad (3.5)$$

Let $a = a_{\text{emb}}(\varphi)$ be the solution of the equation $\tanh(a) = \tanh(l) \cos(\varphi)$, which clearly satisfies $a_{\text{emb}}(\varphi) < a_{\text{max}}(\varphi)$, see Figure 5. Hence, the surfaces provided by Theorems 1 and 2 are properly embedded provided that $a \in [a_{\text{emb}}(\varphi), a_{\text{max}}(\varphi))$. However, on the one hand, it is difficult to know if a value of $a_\varphi \in (0, a_{\text{max}}(\varphi))$ solving the two period problems satisfies the condition (3.5); on the other hand, embeddedness may occur even if the condition (3.5) does not hold. It is expected that there are always values of (a, φ) producing embedded examples solving the two period problems for all $k \geq 3$, and it seems reasonable that this occurs when φ becomes close to $\frac{\pi}{2}$.

3.4. Examples with infinitely many ends. Let us tackle the proof of Theorem 3, which is a particular case of the constructions above for $l = \infty$ (the proof can be easily adapted to the case $l < \infty$). Lemma 3 and the continuity of p_2 imply that, for all $\varphi \in (0, \frac{\pi}{2})$, there are values of $a \in (0, a_{\text{max}}(\varphi))$ such that $p_2(a, \varphi, f(a, \varphi))$ is either equal to 1 or greater than 1. Let us study these two cases:

- If $p_2(a, \varphi, f(a, \varphi)) = 1$, then \tilde{h}_1 and \tilde{h}_3 are contained in vertical planes over asymptotic geodesics of \mathbb{H}^2 in view of item (d) of Lemma 3. This means that

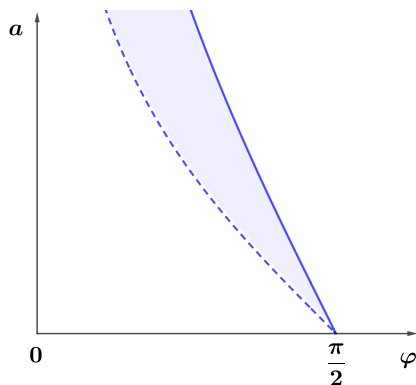


FIGURE 5. The graphic of $a_{\max}(\varphi)$ (solid line) is above the graphic of $a_{\text{emb}}(\varphi)$ (dashed line). The shaded region contains values where embeddedness holds provided that they solve the period problems.

$\tilde{\Sigma}(a, \varphi, f(a, \varphi))$ is contained in the region between these two geodesics, see Figure 6, and mirror symmetries across the corresponding vertical planes span a group of isometries fixing the common point at infinity. This group contains a discrete group of parabolic translations, and gives rise to the 1-parameter family of parabolic ∞ -noids.

- The case $p_2(a, \varphi, f(a, \varphi)) > 1$ occurs in an open subset of Ω , and gives rise to the 2-parameter family of hyperbolic ∞ -noids. The two geodesics of \mathbb{H}^2 containing the projections of \tilde{h}_1 and \tilde{h}_3 do not intersect in this case and successive reflections across their associated vertical planes span a group of isometries containing a discrete group of hyperbolic translations, see Figure 6.

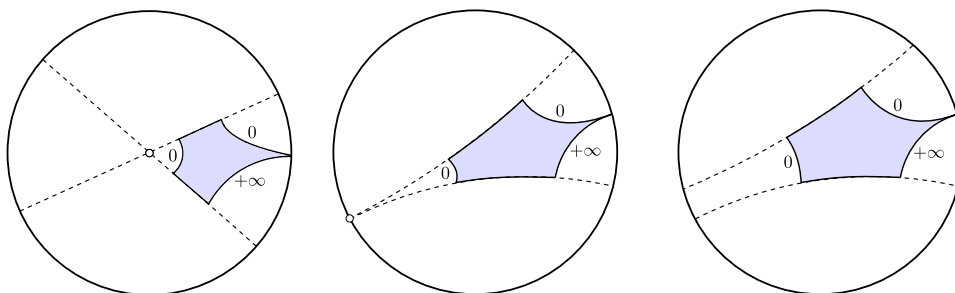


FIGURE 6. The fundamental piece of a 3-noid (left), a parabolic ∞ -noid (middle), and a hyperbolic ∞ -noid (right). The geodesics containing the projection to \mathbb{H}^2 of the curves \tilde{h}_1 and \tilde{h}_3 are represented in dashed line.

Similar arguments as in the proof of Theorems 1 and 2 show that each end of the constructed surfaces is embedded and has finite total curvature, plus the global surface is Alexandrov-embedded. Observe that in the case of hyperbolic ∞ -noids, we can choose a greater than $a_{\text{emb}}(\varphi)$, defined in the previous section, which means that whenever the parameters (a, φ) lie in this open subset of Ω , the reflected surface

is a properly embedded hyperbolic ∞ -noid. In the case of parabolic ∞ -noids, we are not able to guarantee global embededness.

REFERENCES

- [1] P. Collin, H. Rosenberg. Construction of harmonic diffeomorphisms and minimal graphs. *Ann. of Math. (2)*, **172** (2010), no. 3, 1879–1906.
- [2] B. Daniel. Isometric immersions into $\mathbb{S}^n \times \mathbb{R}$ and $\mathbb{H}^n \times \mathbb{R}$ and applications to minimal surfaces. *Trans. Amer. Math. Soc.*, **361** (2009), no. 12, 6255–6282.
- [3] L. Hauswirth, A. Menezes, M.M. Rodríguez. On the characterization of minimal surfaces with finite total curvature in $\mathbb{H}^2 \times \mathbb{R}$ and $\widetilde{PSL}_2(\mathbb{R})$. *Calc. Var. Partial Differential Equations*, **58** (2019), no. 2, Art 80, 24 pp.
- [4] L. Hauswirth, B. Nelli, R. Sa Earp and E. Toubiana. Minimal ends in $\mathbb{H}^2 \times \mathbb{R}$ with finite total curvature and a Schoen type theorem. *Adv. Math.*, **274** (2015), 199–240.
- [5] L. Hauswirth, H. Rosenberg. Minimal surfaces of finite total curvature in $\mathbb{H}^2 \times \mathbb{R}$. *Mat. Contemp.*, **31** (2006), 65–80.
- [6] L. Hauswirth, R. Sa Earp, E. Toubiana. Associate and conjugate minimal immersions in $M \times \mathbb{R}$. *Tohoku Math. J.*, **60** (2008), 267–286.
- [7] J. M. Manzano, F. Torralbo. New examples of constant mean curvature surfaces in $\mathbb{S}^2 \times \mathbb{R}$ and $\mathbb{H}^2 \times \mathbb{R}$. *Michigan Math. J.*, **63** (2014), no. 4, 701–723.
- [8] J. M. Manzano, F. Torralbo. Compact embedded surfaces with constant mean curvature in $\mathbb{S}^2 \times \mathbb{R}$. *Amer. J. Math.* (to appear). Available at arXiv:1802.04070.
- [9] J. M. Manzano, J. Plehnert, F. Torralbo. Compact embedded minimal surfaces in $\mathbb{S}^2 \times \mathbb{S}^1$. *Michigan Math. J.*, **63** (2014), no. 4, 701–723.
- [10] F. Martín, R. Mazzeo, M.M. Rodríguez. Minimal surfaces with positive genus and finite total curvature in $\mathbb{H}^2 \times \mathbb{R}$. *Geom. Top.*, **18** (2014), 141–177.
- [11] L. Mazet. The Plateau problem at infinity for horizontal ends and genus 1. *Indiana Univ. Math. J.* **55** (2006), no. 1, 15–64.
- [12] L. Mazet, M. Rodríguez, H. Rosenberg. The Dirichlet problem for the minimal surface equation –with possible infinite boundary data– over domains in a Riemannian surface. *Proc. London Math. Soc.*, **102** (2011), no. 3, 985–1023.
- [13] L. Mazet, M. Rodríguez, H. Rosenberg. Periodic constant mean curvature surfaces in $\mathbb{H}^2 \times \mathbb{R}$. *Asian J. Math.*, **18** (2014), no. 5, 829–858.
- [14] F. Morabito, M. Rodríguez. Saddle Towers and minimal k -noids in $\mathbb{H}^2 \times \mathbb{R}$. *J. Inst. Math. Jussieu*, **11** (2012), no. 2, 333–349.
- [15] B. Nelli, H. Rosenberg. Minimal surfaces in $\mathbb{H}^2 \times \mathbb{R}$. *Bull. Braz. Math. Soc.*, **33** (2002), no. 2, 263–292.
- [16] J. Plehnert. Surfaces with constant mean curvature $\frac{1}{2}$ and genus one in $\mathbb{H}^2 \times \mathbb{R}$. Preprint (2013). Available at arXiv:1212.2796.
- [17] J. Plehnert. Constant mean curvature k -noids in homogeneous manifolds. *Illinois J. Math.*, **58** (2014), no. 1, 233–249.
- [18] J. Pyo. New complete embedded minimal surfaces in $\mathbb{H}^2 \times \mathbb{R}$. *Ann. Glob. Anal. Geom.*, **40** (2011), no. 2, 167–176.
- [19] J. Pyo, M. Rodríguez. Simply connected minimal surfaces with finite total curvature in $\mathbb{H}^2 \times \mathbb{R}$. *Int. Math. Res. Not.*, **2014** (2014), no. 11, 2944–2954.

DEPARTAMENTO DE GEOMETRÍA Y TOPOLOGÍA,, UNIVERSIDAD DE GRANADA, SPAIN

E-mail address: jcastroinfantes@ugr.es

DEPARTAMENTO DE GEOMETRÍA Y TOPOLOGÍA,, UNIVERSIDAD DE GRANADA, SPAIN

E-mail address: manzanoprego@gmail.com